Communication Networks

Complete Citation: Ziri-Castro, Karla and Scanlon, William and Evans, Noel (2004). Measured pedestrian movement and bodyworn terminal effects for the indoor channel at 5.2 GHz. *European Transactions on Telecommunications*, 14 (6), 529-538. ISSN 1124-318X.

Accessed from USQ ePrints http://eprints.usq.edu.au

Measured Pedestrian Movement and Bodyworn Terminal Effects for the Indoor Channel at 5.2 GHz

KARLA I. ZIRI-CASTRO, WILLIAM G. SCANLON
The Queen's University of Belfast, Ashby Institute, Stranmillis Road, Belfast, BT9 5AH, UK.
w.scanlon @ee.qub.ac.uk

NOEL E. EVANS
University of Ulster, Shore Road, Newtownabbey, Northern Ireland, BT37 0QB, UK.
ne.evans@ulster.ac.uk

Abstract- Human body effects such as antenna-body interaction and scattering caused by pedestrian movement are important indoor radio propagation phenomena at microwave frequencies. This paper reports measurements and statistical analysis of the indoor narrowband propagation channel at 5.2 GHz for two scenarios: a fixed line-of-sight (LOS) link perturbed by pedestrian movement, and a mobile link incorporating a bodyworn terminal moving at 0.5 m/s. Two indoor environments were considered for both types of measurement: an 18-m long corridor and a 42 m^2 office. The fixed-link results show that the statistical distribution of the received envelope was dependent on the number of pedestrians present. However, fading was slower than expected, with an average fade duration of more than 100 ms for a Doppler frequency of 8.67 Hz. For the bodyworn terminal results, mean received power values were dependent on whether or not the user's body obstructed the LOS. For example, in the corridor the average non-line-of-sight (NLOS) pathloss was 5.4 dB greater than with LOS.

1 INTRODUCTION

The recent development and commercialisation of indoor wireless local area network (WLAN) standards at 5 GHz has led to increased interest in propagation studies within this band. Relevant standards currently include HiperLAN type 2 and IEEE 802.11a and feature raw transmission rates of up to 54 Mbps with techniques to mitigate multipath fading such as the use of orthogonal frequency division multiplexing (OFDM). There are a number of significant propagation phenomena present in the indoor environment including multipath fading and human body effects. Human body effects can be divided into temporal variations and shadowing caused by pedestrian movement and antenna-body interaction with bodyworn or handportable terminals [1].

As the elevation of base stations and terminals is much lower in indoor environments than in outdoor communication systems, the propagation loss by body shadowing greatly affects the received signal strength. In addition, pedestrians moving within the environment act as additional scatterers, contributing to multipath fading through a combination of reflection and diffraction mechanisms. Empirical [2], statistical [3], and deterministic [4–5] models for pedestrian effects are available in the literature. However, there are no published systematic studies of the effect of moving pedestrians on the indoor channel at 5.2 GHz. Therefore, this paper reports measurements and statistical analysis of the body shadowing and multipath fading effects associated with pedestrian movement within two indoor environments for a narrowband LOS point-to-point 5.2 GHz link.

An important feature of both current and future WLAN and personal area networking systems is the use of bodyworn and handportable devices. Therefore, there is also a requirement for propagation studies to include the effects of close proximity to the user's body including higher losses and radiation pattern fragmentation [6–8]. In this work, we characterise a narrowband 5.2 GHz link incorporating a bodyworn terminal moving at a moderate walking speed within the indoor environment.

The paper is organised as follows. A short description of the measurement system is given in Section II. Section III describes the propagation environments and the measurement procedure employed. Section IV reports measured pedestrian movement results for the fixed-link, including example raw data and first and second order statistics. The results of the bodyworn terminal study are reported in Section V. Finally, Section VI concludes the paper.

2 MEASUREMENT SYSTEM

A block diagram of the narrowband measurement system is shown in Figure 1. The transmitter (TX) consisted of an R&S SMIQ03B vector signal generator, a GaAs passive frequency doubler (Hittite HMC189MS8), a high efficiency GaAs InGaP power amplifier (Hittite HMC406MS8G), and a sleeve dipole antenna (+2.2 dBi, Mobile Mark model PSTN3-5250). The signal generator was adjusted to deliver +10 dBm of continuous wave at 5.2 GHz to the antenna input port, taking account of cable losses etc. The transmitter system was placed on a wheeled cart to facilitate movement around the different measurement locations. The transmit antenna was vertically polarised and mounted at a height of 1.35 m above floor level.

The receiver module (RX) consisted of a custom 5.2 GHz RF unit, a 12-bit analogue to digital converter (ADC) and a notebook PC for data recording. The receive antenna was a sleeve dipole identical to the one used at the transmitter. The custom RF unit was single conversion with several RF gain stages, filters and logarithmic amplifier detection to deliver an output voltage linear with the received input power in dBm. The unit was built as a portable device enclosed in a 150 x 80 x 50 mm conducting box to facilitate either bodyworn or freestanding use. The specification and measured RF performance parameters of the RF unit are given in Table 1. The received power indication from the RF unit was sampled at a minimum interval of 5 ms using the ADC and the results stored on the notebook PC.

3 EXPERIMENTAL SET-UP

3.1 Measurement locations

Two in-building locations were selected for the experimental measurements, see Figure 2; both were situated on the fifth floor of a university building. Location 1 was a 1.3 m by 18 m corridor, and location 2 was a 6 m by 7 m rectangular office. In both cases, the walls were constructed from painted concrete blocks and the floor was covered with commercial grade polypropylene carpet. The ceiling was suspended at a height of 2.5 m and was composed of mineral tiles and recessed louvered luminaires. The ceiling void above was 0.5 m high. The office location had a wall-mounted chalkboard and half height windows along one wall, see Figure 2.

The location of the TX cart within each area is also shown in Figure 2 and was fixed for all of the measurements reported in this paper. In the corridor, the TX cart was placed at 1.75 m and 0.67 m from the walls, while in the room it was placed at 0.3 m and 3.5 m from the walls. The offset dimensions are measured relative to the antenna position on the cart. During the experiments, both locations were cleared of furniture and obstructions to allow the free movement of the user and pedestrians.

3.2 Measurement procedure

Two types of measurements were performed, the first was for a fixed LOS point-to-point link with groups of 1, 2 or 3 pedestrians walking simultaneously, and the second was for a bodyworn receiver, with the user walking at approximately 0.5 m/s. There were no pedestrians present during the bodyworn receiver measurements.

For the fixed-link measurements, the receiver system was set on a wooden support with the antenna fixed at 0.9 m above floor level in a predetermined position within each measurement location. Four different scenarios were considered within each location: the empty room, a single pedestrian, and a group of 2 and a group of 3 pedestrians walking simultaneously, at a constant speed of approximately 0.5 m/s. In location 1, the receiver was positioned at the end of the corridor, 18 m from the TX, 0.5 m and 0.6 m from the walls. In this location, the pedestrians walked along the LOS as shown in Figure 2a. In location 2, the receiver was situated 5 m from the TX, 0.5 m and 3.5 m from the walls. Here, the pedestrians walked perpendicular to the link across the midline of the room, shown dotted in Figure 2b. The geometry in location 2 was such that a single NLOS event occurred in the temporal profile as the pedestrians' bodies obstructed the direct ray to the transmitter. The sampling interval for the fixed-link measurements was 5-ms, equating to a pedestrian movement, or scatterer shift, of less than $\lambda/23$ at a pedestrian speed of 0.5 m/s, where $\lambda = 5.8$ cm is the carrier wavelength. The measured received power results included both transmit and receive antenna gains.

For the bodyworn measurements, the receiver RF unit was positioned towards the front of the user's body at the hip. The ADC and notebook PC were placed in a backpack carried by the user. Two types of measurements were recorded in both locations: LOS, where the user was walking towards the TX, and NLOS where the user was walking away. In location 1 (corridor) the user walked along the middle line only,

shown dotted in Figure 2a. However, in location 2, a total of 14 parallel trajectories were considered, each one separated by 0.5 m. Figure 2c shows two of the 14 trajectories: centre (across the middle of the room) and the edge (close to one wall). The sampling interval for the bodyworn terminal measurements was 10-ms allowing a measurement resolution better than λ/11 for a user speed of 0.5 m/s. The measured received power results include both transmit and receive antenna gains, losses in the user's body and radiation pattern distortion effects.

4 FIXED-LINK RESULTS

4.1 Location 1 (corridor)

Figure 3 shows the received power profiles for the fixed-link measurements with up to 3 pedestrians walking simultaneously along the corridor. In the case of a single pedestrian, the received signal has two strong faded areas, the first one between 0 s and 10 s and a second one between 33 s and 35 s. This is due to the close proximity of the pedestrian body to the TX and the RX, respectively. The two-pedestrian plot has a similar trend with most fading occurring when the pedestrians are close to the test antennas. In the three-pedestrian case, fade events occur throughout the recorded profile as the pedestrians move along the corridor. Qualitatively, the profiles in figure 3 indicate that the degree of fading experienced by the fixed-link is strongly dependent on the number of pedestrians moving in the corridor. Although they are not completely symmetric, all of the pedestrian profiles in Figure 3 exhibit similar fading patterns at both ends of the link. Table 2 shows the mean received power, dynamic range (difference between maximum and minimum received power), and standard deviation for the received envelope in the fixed-link measurements. The mean received power for the single pedestrian case, –56.3 dBm, was 2.5 dB higher than that recorded for the empty corridor, suggesting that the receiver was positioned at the location of a fade. However, due to the increased obstruction area, the mean received power for the two and three pedestrian cases were 3 dB and 4.3 dB lower than the empty corridor scenario, respectively.

The cumulative distribution function (CDF) for the received envelope was calculated for all the measured fixed-link scenarios in location 1 and compared with theoretical Lognormal, Rayleigh and Rice distributions, see Figure 4. Three different K factors where considered for the Rice distribution: K = 3 dB, K = 7 dB, and K = 15 dB. The Rice K factor is defined as the power ratio of the dominant (specular) component of the signal and the multipath (random) components, as follows:

$$K(dB) = 10\log\left(\frac{r_s^2}{2\sigma^2}\right) \quad (1),$$

where r_s is the envelope of the dominant component and σ is the standard deviation of the envelope the multipath component.

The single-pedestrian CDF tends to a Rice distribution with a K factor of between 3 dB and 7 dB. The two-pedestrian CDF is approximately Rayleigh, while the three-pedestrian CDF is between the Lognormal and the Rayleigh distribution.

The level-crossing rate (LCR), defined as the rate at which the envelope crosses a specified level in a positive-going direction, and average fade duration (AFD), the average time for which the received envelope is below that specified level, were also calculated for the fixed-link results in location 1, see Figure 5. In all cases, LCR and AFD results were computed for levels from –20 to 10 dB with respect to the relevant local mean, in 0.05 dB steps. The LCR and AFD results were compared to theoretical Rayleigh and Ricean (K = 3 dB, 7 dB, and 15 dB) distributions with a maximum Doppler frequency (f_m) of 8.67 Hz, for a scatterer speed of 0.5 m/s.

The theoretical LCR for a Rice distribution [9] is given by:

$$L_R = \sqrt{2\pi(K+1)}\, f_m \rho e^{-K-(K+1)\rho^2} I_0\left(2\rho\sqrt{K(K+1)}\right) \quad (2),$$

where K is the Rice factor, ρ is the value of a specified level R normalized to the root-mean-square (rms) amplitude of the fading envelope, and $I_0(.)$ designates the zeroth-order modified Bessel function of the first kind. For Rayleigh fading (K=0), this expression simplifies to:

$$L_R = \sqrt{2\pi}\, f_m \rho e^{-\rho^2}. \quad (3)$$

If the envelope has the Rice distribution, the AFD is given by:

$$\bar{\tau} = \frac{1 - Q\left(\sqrt{2K}, \sqrt{2(K+1)\rho^2}\right)}{\sqrt{2\pi(K+1)}\, f_m \rho e^{-K-(K+1)\rho^2} I_0\left(2\rho\sqrt{K(K+1)}\right)} \quad (4)$$

where $Q(a,b)$ is the Marcum Q function. If the envelope is Rayleigh distributed, then:

$$\bar{\tau} = \frac{e^{\rho^2} - 1}{\rho f_m \sqrt{2\pi}}. \quad (5)$$

Figure 4 shows that the number of pedestrians moving within the corridor significantly affects the second order statistics of the channel. However, both the LCR and AFD distributions recorded for pedestrian movement within the corridor exhibit slower fading characteristics than would be expected for a Rayleigh or Rice distribution at a scatterer speed of 0.5 m/s.

4.2 Location 2 (office)

Figure 6 shows the received power profiles for the scenario illustrated in Figure 2b. Here, in contrast to the corridor measurements, the single pedestrian or group of pedestrians walked perpendicular to the fixed-link. The temporal profiles for the dynamic scenarios exhibit a single NLOS event due to the obstruction caused by the pedestrians' bodies at approximately 6 s. This NLOS event introduces a fade of almost 10 dB in the received signal. However, this is not the only human body effect observed. There was significant envelope variation throughout the entire measurement period in all of the

dynamic profiles even when the direct ray was not obstructed. The difficulty in maintaining a constant pedestrian speed is also highlighted by Figure 6. For example, the fade caused by obstructing the LOS occurs later for the three-pedestrian case. Presumably, this is due to the difficulties encountered by the test volunteers as they tried to move across the room in tandem. The mean received power, dynamic range, and standard deviation for all the location 2 scenarios are shown in Table 2. Although the mean received powers are similar, the dynamic range and standard deviation both increase monotonically with the number of pedestrians present.

The CDFs for fixed-link measurements in location 2 are shown in Figure 7. All of the scenarios, apart from the empty room, tended to be Rice distributed. The single-pedestrian scenario followed the Rice distribution with K between 7 and 3 dB. The two-pedestrian and the three-pedestrian scenarios are similar to each other, with K ranging from 3 to 0 dB. All the fading signals measured are predominantly Rice distributed because of the presence of a stronger direct ray component, which is attenuated only when the pedestrians physically block the LOS. The reduction in the Rice factor as the number of pedestrians present increases may be due to the higher probability of obstructing both the direct ray and any strong multipath components.

5 BODYWORN TERMINAL RESULTS

5.1 Location 1 (corridor)

Figure 8 shows the received power profiles for the bodyworn terminal measurements where the user was walking along the middle of the corridor. Note that the measurements were recorded as a time series and the conversion to distance assumed a constant walking speed. This limitation means that the profiles in Figure 8 can only be qualitatively compared in terms of distance between the antennas. However, the NLOS plot does suggest an increased rate of multipath fading and, at distances close to the transmitter, blocking due to the user's body itself. Note that the NLOS results are consistently lower than LOS due to the attenuation of the direct ray by the user's body. Table 3 gives the summary parameters for these results, including the calculated power decay index, n. The decay index is similar for both NLOS and LOS cases, and is much less than the free-space value of 2.0. However, the shadowing effect of the user's body has led to a 5.4 dB reduction in average received power for the NLOS results.

The bodyworn receiver CDFs for the received power envelope in location 1 were compared with the theoretical Rayleigh, Rice, and lognormal distributions, see Figure 9. Both the LOS and the NLOS profiles are lognormally distributed due to the path-loss attenuation associated with the receiver moving along the corridor from, or to, the TX.

The LCR and AFD distributions were computed for the bodyworn terminal results in location 1 (Figure 10), assuming a maximum Doppler frequency, f_m, of 8.67 Hz (for a receiver speed of 0.5 m/s). The peak of the measured NLOS LCR curve was higher and more similar to the Rayleigh distribution than that of the LOS curve, confirming that multipath contributions were dominant in the received signal. The AFD results indicate that the bodyworn LOS fade duration was, in general, longer than for NLOS. Inspection of the raw fading profiles confirmed that the bodyworn receiver measured results experienced significantly more fading that the fixed-link results reported in Section IV. This suggests that the changes in antenna-body interaction associated with walking led to more rapid envelope variation.

5.2 Location 2 (office)

In location 2, the bodyworn terminal received power profiles for both LOS and NLOS (14 in each case) were averaged using a 1-Hz zero-phase recursive digital low pass filter. The filter was based on a recursive (IIR) filter and it attempted to minimise start-up transients by adjusting initial conditions to match the DC component of the signal. The effective averaging distance was 0.5 m (8.7 λ). Table 4 gives a summary of the mean received power levels for the office measurements. The highest local mean values were found close to the transmitter location (–32.7 dBm for LOS and –37.4 dBm for NLOS). Overall (i.e., for all 14 trajectories measured), the NLOS results were 3.8 dB lower than LOS. However, the effect of the user's body blocking the direct ray was most noticeable for the trajectories recorded at the centre of the room. Here, the NLOS signal was 12.0 dB lower than LOS. At the room edge, where the effect of the direct ray is reduced and multipath components can become dominant, the situation is reversed, as the LOS results were 1.5 dB lower than NLOS.

The location 2 bodyworn receiver CDFs were calculated over the entire 14 measurement profiles for both LOS and NLOS cases Figure 11 shows the results for the centre trajectory. Both LOS and NLOS datasets tend to be more lognormally distributed, rather than Rayleigh or Rice, despite the relatively short distances involved (a maximum of 5.5 m for each trajectory). However, as in location 1, the LCR distribution (Figure 12) shows that the peak crossing-rate for the NLOS bodyworn receiver data was higher than that for LOS. This suggests an increased multipath contribution in the received signal. In addition, the AFD distribution for both locations shows that the fading associated with the bodyworn receiver is much faster than that for the fixed-link with pedestrian movement (Figure 5).

6 Conclusions

The results presented in this paper firmly demonstrate that human body propagation effects are significant for the indoor communications channel at 5 GHz. The effect of pedestrian movement was studied using a LOS narrowband 5.2 GHz link within two

contrasting locations: a long narrow corridor and a small office. In the corridor, the distribution of the received envelope varied with the number of pedestrians present. However, fading was relatively slow given the maximum Doppler frequency of 8.67 Hz; the LCR was less than 3 Hz and the AFD typically more than 200 ms, regardless of the number of pedestrians. In the office environment the pedestrian movement was perpendicular to the LOS and the envelope tended to be Rice distributed, albeit with a low K of between 7 dB (single pedestrian) and 3 dB (2 and 3 pedestrians).

Bodyworn terminal effects were studied in the absence of pedestrian movement in both environments. Local mean values were dependent on whether or not the user's body obstructed the LOS to the transmitter with between 3.8 dB (office) and 5.4 dB (corridor) of additional shadow loss. However, in the office, the difference between LOS and NLOS conditions was strongly dependent on the location within the room. Although the bodyworn terminal envelopes were all lognormally distributed, there was evidence of increased multipath fading for the NLOS results in both locations. Second-order statistical analysis showed that the NLOS results had consistently shorter fade durations and higher crossing rates than for LOS.

For the first time, we have presented a systematic investigation of human body effects on the 5 GHz indoor radio channel. The statistical results presented will be of use to system designers and researchers for performance modelling and evaluation. Future work will involve additional propagation studies in more complex building structures with a variety of controlled and uncontrolled pedestrian traffic conditions.

REFERENCES

[1] W. G. Scanlon, and N. E. Evans. Numerical analysis of bodyworn UHF antenna systems. *IEE Electronics & Communication Engineering Journal*, Vol. 13, No. 2, pages 53–64, April 2001.

[2] R. J. C. Bultitude. Measurement, characterization and modelling of indoor 800/900 MHz radio channels for digital communications. *IEEE Communication Magazine*, Vol. 25, No. , pages 5-12, June 1987.

[3] J. A. Roberts, and J. R. Abeysinghe. A two-state Rician model for predicting indoor wireless communication performance. In *IEEE International Conference on Communications*, Seattle, WA, pages 40-43, June 1995.

[4] S. Obayashi, and J. Zander. A body-shadowing model for indoor radio communication environments. *IEEE Transactions on Antennas and Propagation*, Vol. 46, No. 6, pages 920–927, June 1998.

[5] F. Villanese, W. G. Scanlon, N. E. Evans, and E. Gambi. Hybrid image/ray-shooting UHF radio propagation predictor for populated indoor environments. *Electronic Letters*, Vol. 35, No. 21, pages 1804–1805, Octobre 1999.

[6] J. Toftgard, S. N. Hornsleth, and J. B. Andersen. Effects on portable antennas of the presence of a person. *IEEE Transactions on Antennas and Propagation*, Vol. 41, No. 6, pages 739–746, 1993.

[7] H.-R. Chuang. Human operator coupling effects on radiation characteristics of a portable communication dipole antenna. *IEEE Transactions on Antennas and Propagation*, Vol. 42, No. 4, pages 556-560, 1994.

[8] F. L. Lin and H.-R. Chuang. Performance evaluation of a portable radio close to the operator's body in urban mobile environments. *IEEE Transactions on Vehicular Technology*, Vol. 49, No. 2, pages 614–621, 2000.

[9] G. Stüber. *Principles of Mobile Communication*. Kluwer Academic Publishers, 2001.

Table 1: Specification and measured performance for receiver custom RF unit.

Parameter		Comment
Intermediate Frequency (IF)	915 MHz	Single conversion
IF bandwidth	25 MHz	Nominal
Front end gain	20.2 dB	Includes IL for bandpass filters and mixer
Calculated Noise Figure	4 dB	
Effective noise floor	–96 dBm	
IF Detector type	Log amp	Analog Devices AD8313
Range of input power for linear output	–23 dBm to –88 dBm	65 dB dynamic range (+/- 1 dB error)
Output sensitivity	46 mV/dB	Vout: 1.2 V to 4.6 V
Output jitter	+/- 2 mV	0.04 dB

Table 2: Mean received power, dynamic range, and standard deviation for the fixed-link measurements.

Location	Scenario	Mean Received Power (dBm)	Dynamic Range (dB)	Standard Deviation (dB)
1: Corridor	Empty	–58.8	1.1	0.3
	1 Pedestrian	–56.3	16.0	3.5
	2 Pedestrians	–61.8	19.5	3.8
	3 Pedestrians	–63.1	19.1	4.1
2: Office	Empty	–53.4	1.0	0.2
	1 Pedestrian	–54.2	10.0	1.7
	2 Pedestrians	–53.9	10.6	2.0
	3 Pedestrians	–53.7	11.6	2.1

Table 3: Summary statistics and estimated path loss index, n, for bodyworn terminal measurements in Location 1.

Scenario	Mean Received Power (dBm)	Dynamic Range (dB)	Standard Deviation (dB)	Power Decay Index, *n*	rms error for *n* (dB)
LOS	-49.6	35.3	6.9	1.27	5.35
NLOS	-55.0	39.5	6.9	1.23	5.52

Table 4: Mean received power levels for the bodyworn measurements in location 2 (office).

Scenario	Mean received power (dBm)	Body shadowing effect (dB)
Office all LOS	–46.6	
Office all NLOS	–50.4	3.8
Office centre LOS	–43.4	
Office centre NLOS	–55.4	12.0
Office edge LOS	–54.6	–1.5
Office edge NLOS	–53.1	(NLOS>LOS)

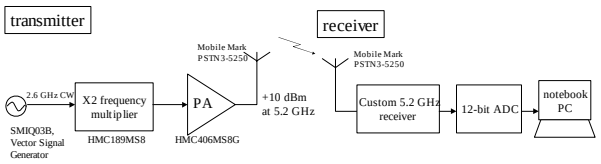

Figure 1: Block diagram of narrowband 5.2 GHz measurement system.

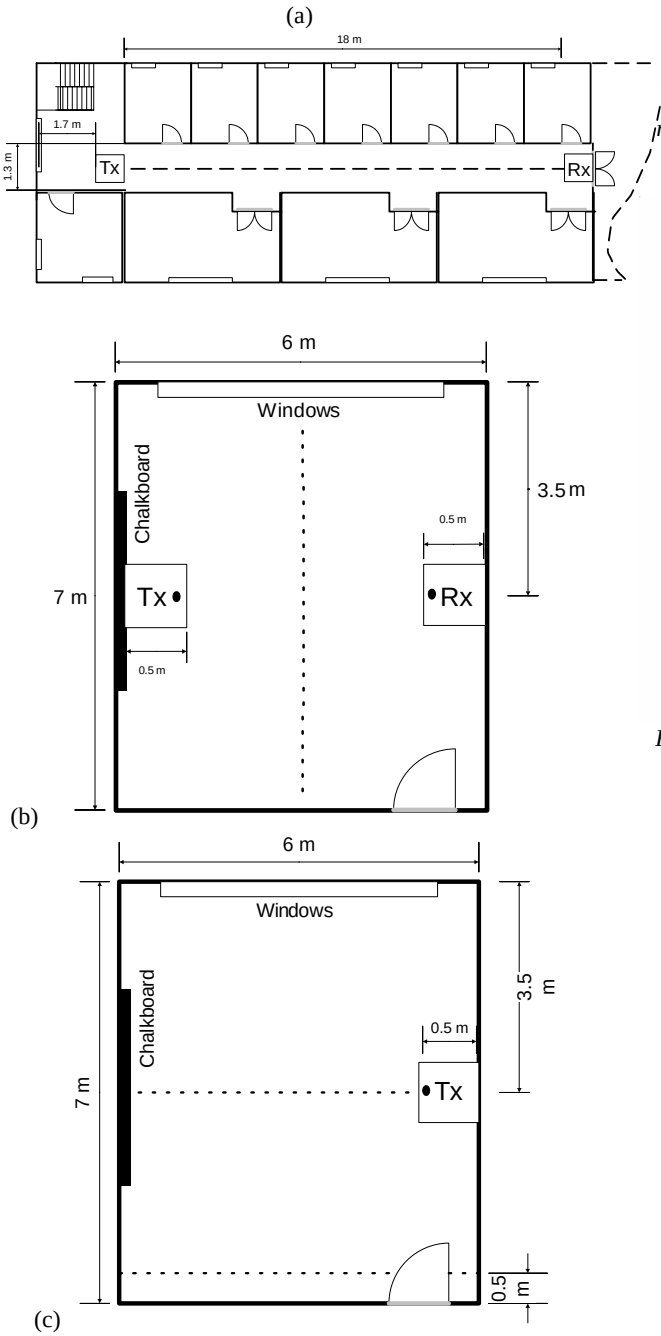

Figure 2: Layout of measurement locations. Pedestrian / bodyworn receiver trajectories are shown dotted: a) location 1, corridor, b) location 2, office, c) location 2 setup for the bodyworn receiver measurements.

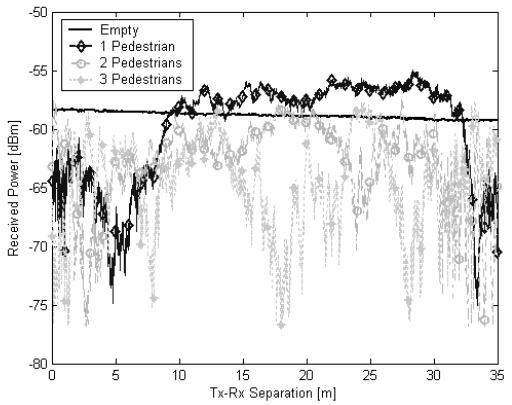

Figure 3: Received power profiles for the fixed-link measurements in location 1 (pedestrians walking at 0.5 m/s along the LOS).

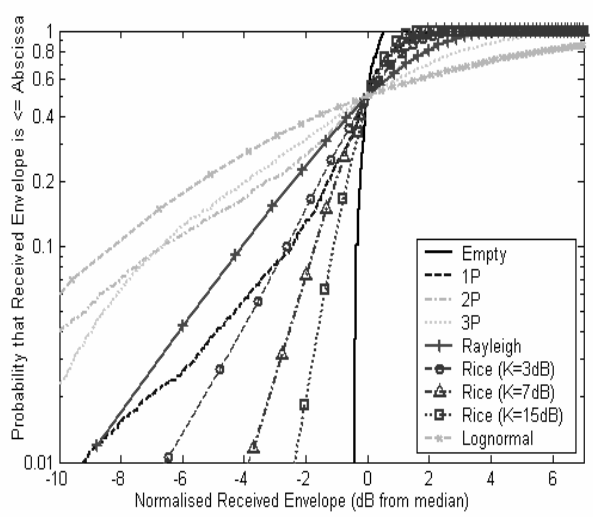

Figure 4: CDF for location 1 fixed-link results. Lognormal, Rayleigh and Rice distributions are shown for reference.

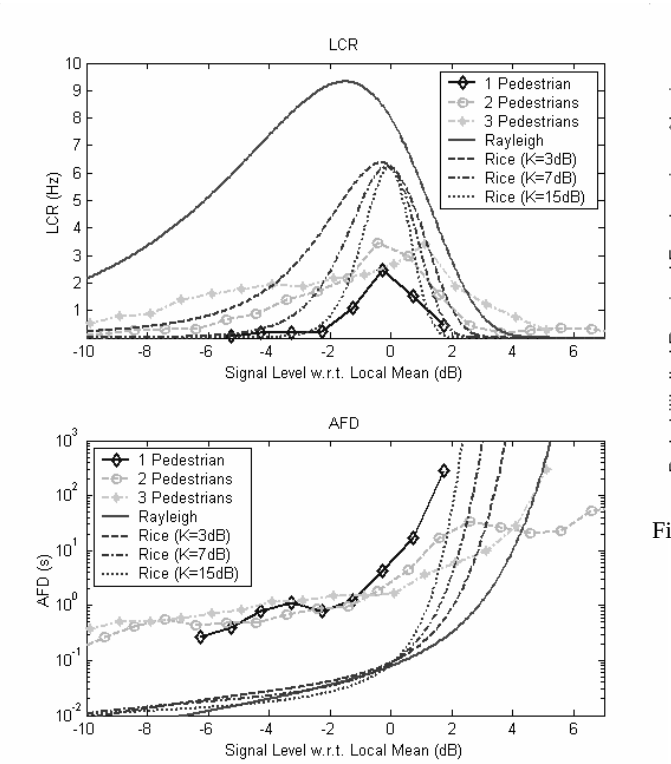

Figure 5: LCR and AFD results with respect to (w.r.t.) local mean for location 1 fixed-link. Rayleigh and Rice distributions are shown for reference.

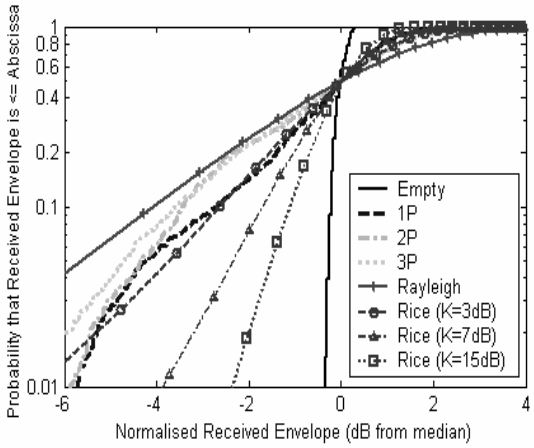

Figure 7: CDF for location 2 fixed-link results. Rayleigh and Rice distributions are shown for reference.

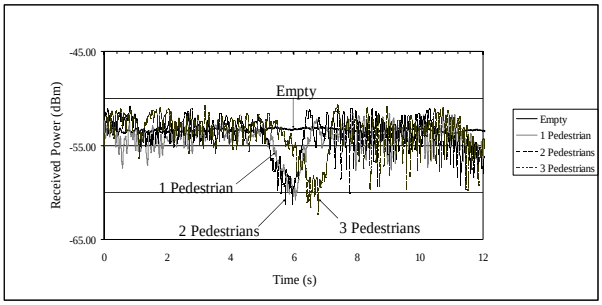

Figure 6: Received power profiles for the fixed-link measurements in location 2 (pedestrians walking at 0.5 m/s perpendicular to the link). [remove box and re-plot in MATLAB with B&W symbols]

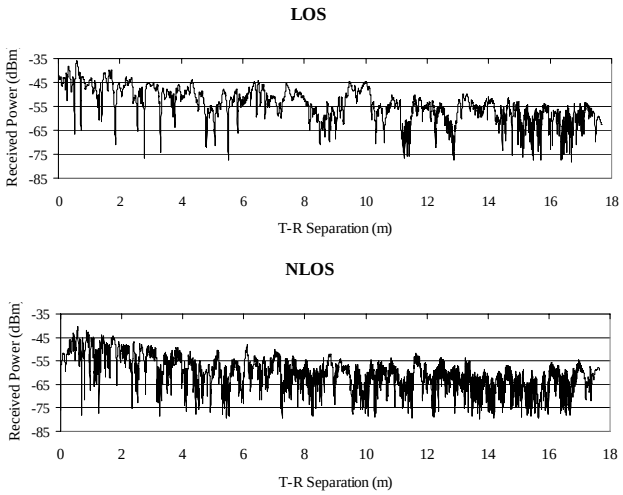

Figure 8: Received power profile for Location 1, upper plot is for LOS (user walking towards the transmitter) and the lower plot is for NLOS (walking away).

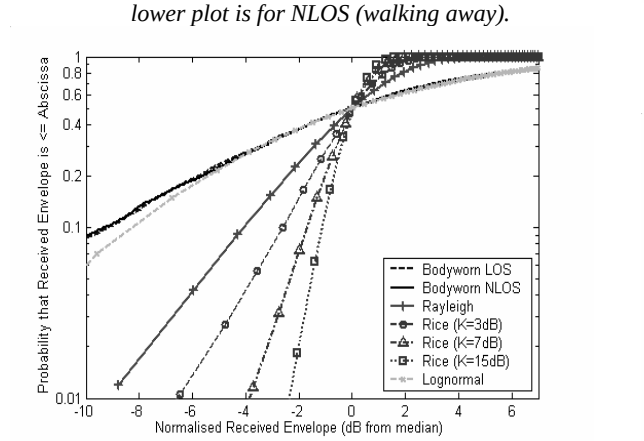

Figure 9: CDF for location 1 bodyworn terminal results. Lognormal, Rayleigh and Rice distributions are shown for reference.

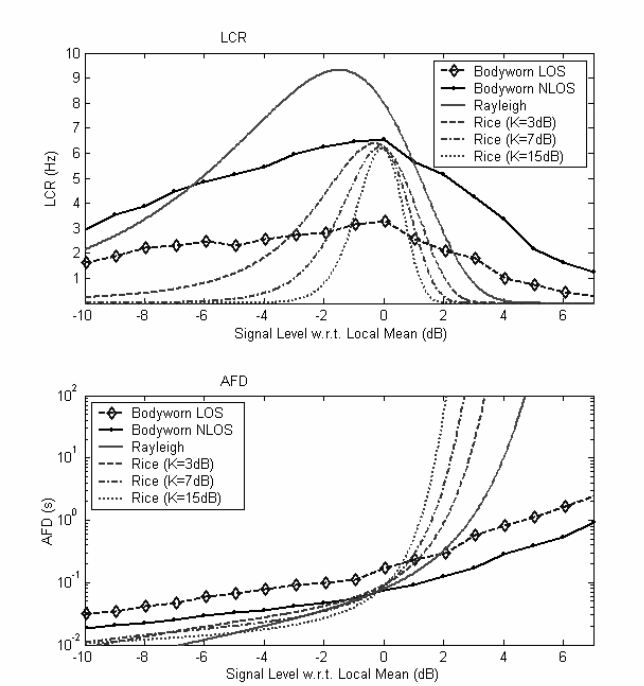

Figure 10: LCR and AFD results with respect to (w.r.t.) local mean for location 1 bodyworn terminal results. Rayleigh and Rice distributions are shown for reference.

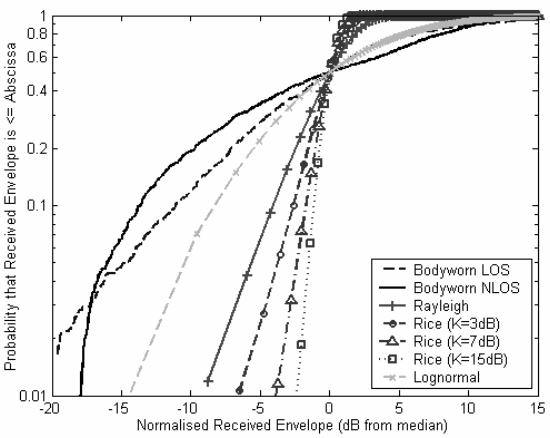

Figure 11: CDF for location 2 bodyworn terminal results. Lognormal, Rayleigh and Rice distributions are shown for reference.

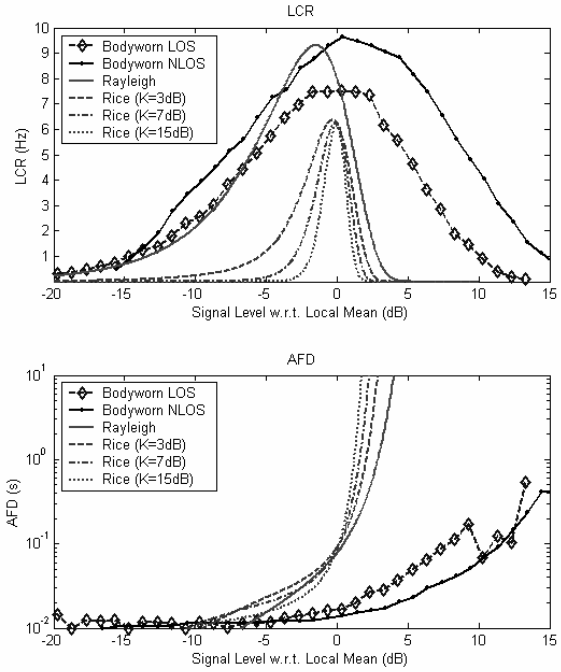

Figure 12: LCR and AFD results for location 2 bodyworn terminal results. Rayleigh and Rice distributions are shown for reference.